HHS Public Access

Author manuscript

Neurobiol Dis. Author manuscript; available in PMC 2023 December 06.

Published in final edited form as:

Neurobiol Dis. 2023 November ; 188: 106331. doi:10.1016/j.nbd.2023.106331.

Experimental traumatic brain injury increases epichaperome formation

Sarah E. Svirsky[a,b,1], **Youming Li**[a,1], **Jeremy Henchir**[a,1], **Anna Rodina**[c,2], **Shaun W. Carlson**[a,1], **Gabriela Chiosis**[c,2], **C. Edward Dixon**[a,b,d,*,1]

[a]Center for Neuroscience, University of Pittsburgh, Pittsburgh, PA, USA

[b]Department of Neurological Surgery, University of Pittsburgh Medical Center, Pittsburgh, PA, USA

[c]Chemical Biology Program, Memorial Sloan Kettering Cancer Center, New York, NY, USA

[d]V.A. Pittsburgh Healthcare System, Pittsburgh, PA, USA

Abstract

Under normal conditions, heat shock proteins work in unison through dynamic protein interactions collectively referred to as the “chaperome.” Recent work revealed that during cellular stress, the functional interactions of the chaperome are modified to form the “epichaperome,” which results in improper protein folding, degradation, aggregation, and transport. This study is the first to investigate this novel mechanism of protein dishomeostasis in traumatic brain injury (TBI). Male and female adult, Sprague-Dawley rats received a lateral controlled cortical impact (CCI) and the ipsilateral hippocampus was collected 24 h 1, 2, and 4 weeks after injury. The epichaperome complex was visualized by measuring HSP90, HSC70 and HOP expression in native-PAGE and normalized to monomeric protein expression. A two-way ANOVA examined the effect of injury and sex at each time-point. Native HSP90, HSC70 and HOP protein expression showed a significant effect of injury effect across all time-points. Additionally, HSC70 and HOP showed significant sex effects at 24 h and 4 weeks. Altogether, controlled cortical impact significantly increased formation of the epichaperome across all proteins measured. Further investigation of this pathological mechanism can lead to a greater understanding of the link between TBI and increased risk of neurodegenerative disease and targeting the epichaperome for therapeutics.

*Corresponding author at: Center for Neuroscience, University of Pittsburgh, Pittsburgh, PA, USA. ses240@pitt.edu (S.E. Svirsky), yol8@pitt.edu (Y. Li), jjhst22@pitt.edu (J. Henchir), rodinaa@mskcc.org (A. Rodina), carlsons@pitt.edu (S.W. Carlson), chiosisg@mskcc.org (G. Chiosis), dixoec@upmc.edu (C.E. Dixon).

[1]4401 Penn Ave, Pittsburgh, Pennsylvania 15,224

[2]1275 York Avenue, New York, New York, 10,065

Authorship contribution statement

Sarah E. Svirsky: investigation, data analysis, manuscript drafting and revision; **Youming Li:** tissue processing and immunoblot methodology; **Jeremy Henchir:** surgical methodology; **Anna Rodina:** data interpretation, manuscript critical review; **Shaun W. Carlson:** data interpretation, manuscript critical review and revision; **Gabriela Chiosis:** data interpretation, manuscript critical review; **C. Edward Dixon:** conceptualization, project supervision, project administration, manuscript critical review and revision.

Supplementary data to this article can be found online at https://doi.org/10.1016/j.nbd.2023.106331.

Keywords

Traumatic brain injury; Epichaperome; hippocampus; Neurodegeneration

1. Introduction

A single traumatic brain injury (TBI) significantly increases the risk for developing neurodegenerative disease later in life (Brett et al., 2022; Graham and Sharp, 2019). It is postulated that TBI induces similar pathological mechanisms of canonical protein pathways implicated in Alzheimer's disease, Parkinson's Disease and Amyotrophic Lateral Sclerosis, contributing to onset and progression (Cruz-Haces et al., 2017). Secondary injury processes such as excitotoxicity, apoptosis, neuro-inflammation, oxidative stress occur early after a TBI and persist chronically (Bramlett and Dietrich, 2015; Simon et al., 2017). These hallmark secondary processes contribute to improper folding, degradation, aggregation and transport of proteins (Smith et al., 2003). This can lead to aberrant synaptic communication and disrupted neuronal circuitry, leading to impaired cognition. Understanding mechanisms that link secondary injury processes to dysfunctional proteostasis can lead to targeted therapies for the treatment of TBI.

Heat shock proteins (HSP), also known as chaperones, are responsible for aiding in protein folding, degradation, dis-aggregation and transport within the neuron (Balchin et al., 2016; Kaushik and Cuervo, 2015; Lindberg et al., 2015). The "chaperome," is a collective of HSPs which work together in unison, through dynamic protein interactions. These interactions aren't based on individual protein expression, but rather through the strength and number of interactions (Inda et al., 2020; Rodina et al., 2016; Tai et al., 2016). However, due to pathological mechanisms, such as cellular stress, this functional chaperome is modified to form the "epichaperome." Specifically, proteomic imbalance due to increased protein synthesis, high metabolic burden, hypoxic and acidic conditions, and production of reactive oxygen species increases the demand and ultimately overwhelms the chaperome to function properly, leading to the formation of the epichaperome (Ginsberg et al., 2023; Harper and Bennett, 2016; Joshi et al., 2018). This form is maladaptive and has been shown to contribute to network-wide dysfunction in Alzheimer's Disease and tumor growth in various cancers (Inda et al., 2020; Rodina et al., 2016; Tai et al., 2016). In both human and pre-clinical models of disease, epichaperome-mediated dysfunctions compromise whole brain networks through disrupting synaptic plasticity, cellular communication, protein translation, cell cycle, axon guidance, metabolic processes and inflammation, ultimately resulting in worsened cognitive performance (Ginsberg et al., 2022; Ginsberg et al., 2021; Inda et al., 2020; Kishinevsky et al., 2018; Rodina et al., 2016). Further work has shown that functional imbalances in synaptic protein networks are reverted to normal upon pharmacologic epichaperome inhibition, demonstrating a causal link between dysfunctions in neuronal protein pathways and the epichaperome in an experimental model of Alzheimer's disease (AD).

As critical hub proteins, heat shock protein 90 (HSP90) and heat-shock cognate 70 (HSC70) are the central proteins involved in the pathological formation of the epichaperome (Chiosis

et al., 2023; Inda et al., 2020; Kishinevsky et al., 2018; Rodina et al., 2016; Yan et al., 2020) and are linked together by HSP-organizing protein (HOP). Once HSP90 and HSC70 are biochemically altered into the epichaperome epicenter, importantly, these proteins both lose their normal physiological function of proper protein production, but also recruit a wide range of co-chaperones into the scaffold, perpetuating pathological progression. In their role as hub proteins, HSP90 and HSC70 are representative markers of the large assembly of pathological epichaperome complex, comprised of an entire network of aberrantly interacting chaperone proteins (Chiosis et al., 2023; Inda et al., 2020; Kishinevsky et al., 2018; Rodina et al., 2016).

Previous experimental TBI models have only evaluated monomeric shifts in mRNA and protein expression of HSP proteins in the hours to days after injury, with recovery to baseline levels generally within 24 hours (Chen et al., 1998; Dutcher et al., 1998; Lai et al., 2004; Michael et al., 2005; Raghupathi et al., 1995; Seidberg et al., 2003; Truettner et al., 1999, 2007). Pharmacological and genetic manipulations of monomeric levels of HSP70 can attenuate a range of neuropathological responses (Kim et al., 2013, 2015), however no study has evaluated therapeutic potential beyond 14 days post-injury. Currently, there is a limited understanding of the long-term consequences role these proteins have in the pathogenesis of neurodegenerative diseases. Furthermore, as previously mentioned, the development of the TBI epichaperome may occur independent of monomeric protein expression. Only a minority of HSP90 and HSC70 is incorporated into the epichaperome, so monomeric forms of these proteins appear to operate in parallel (Rodina et al., 2016). Previous studies that assess only monomeric forms, do not fully capture the pathological nature of the same proteins within the epichaperome complex. Even the sequestering of a small proportion of these proteins into the epichaperome can have large consequences on protein homeostasis.

This study is the first to our knowledge to examine the effect of TBI on the formation of the epichaperome complex. Dynamic protein complexes typically disassemble under native protein chromatography, however the epichaperome can be detected as high molecular weight (HMW) complexes under these conditions (Rodina et al., 2016). We will measure monomeric and HMW expression of HSP90, HSC70 and HOP to determine epichaperome expression in the ipsilateral hippocampus 24 hours to 4 weeks after controlled cortical impact (CCI). Given the relationship between secondary processes after TBI, cellular stress and epichaperome formation, we hypothesize that CCI will increase epichaperome complex formation across all time points for both male and female animals.

2. Methods

2.1. Animals and surgical procedures

All experimental procedures were approved by the University of Pittsburgh Institutional Animal Care and Use Committee in accordance with the guidelines established by the National Institutes of Health in the Guide for the Care and Use of Laboratory Animals. Animals were housed up to two rats per cage in the University of Pittsburgh vivarium with a 12:12 light/dark photoperiod (lights on at 7:00 a.m.) and provided food and water *ad libitum*. Animals were also monitored daily by veterinary technicians.

A total of 48 male and 48 female adult, Sprague-Dawley rats (250–350 g, Envigo, Indianapolis, IN) were used for this study, with 6 animals per injury group per time-point. In females, vaginal lavage and estrous cycle determination was conducted once immediately prior to surgical procedures, using methods previously described (Cora et al., 2015; Fortress et al., 2019). Animals were initially anesthetized with 4% isoflurane in 2:1N_2O/O_2 and maintained using 2% isoflurane in 2:1 N_2O/O_2. Following intubation, rats were placed on a thermal blanket to regulate body temperature (37 °C). The animal's head was placed in a stereotaxic frame and a parasagittal craniectomy (center of craniectomy at AP: +4.0mm, L: +2.8mm from lambda) 8mm in diameter exposed the brain to allow access for the impactor tip (6 mm flat tip) of the CCI device (Pittsburgh Precision Instruments Inc., Pittsburgh PA). CCI at a depth of 2.5 mm at 4 m/s was carried out. After injury, the surgical area was closed by silk sutures and animal recovery was monitored by measuring righting reflexes. Sham (control) injury animals were subjected to identical anesthesia and surgical procedures but did not receive a TBI. There were no significant differences in righting times between male and female animals after either sham or CCI injury (Supplemental Fig. 1A). Furthermore, there were no significant differences between estrous phases between female animals between the sham and CCI injured group (Supplemental Fig. 1B).

2.2. Tissue preparation

At 24 hours or 1, 2, or 4 weeks post-injury, animals received an overdose of sodium pentobarbital (intraperitoneally, 100 mg/kg Fatal-plus, Vortech Pharmaceuticals, Dearborn, MI) and were rapidly decapitated. Ipsilateral hippocampus was rapidly dissected on a chilled ice plate and immediately frozen in liquid nitrogen and stored at −80 °C. As adapted from in Inda et al., 2020, tissue was homogenized using a dounce homogenizer in lysis buffer (20 mM Tris pH 7.4, 20 mM KCl, 5 mM MgCl2, 0.01% NP40 buffer with protease/phosphatase inhibitors). Homogenates were incubated on ice for 30 min and vortexed. Proteins were extracted by freeze-thaw procedures with liquid nitrogen. Lysates were centrifuged at 13,200 $\times g$ for 30 min at 4 °C. Protein concentration was measured with a bicinchoninic acid protein assay kit (Thermo Scientific, Pittsburgh PA) using a 96-well microplate reader (Biotek, Winooski, VT).

2.3. Native-polyacrylamide gel electrophoresis (PAGE) Western Blot

20 μg of hippocampal total protein in 2× loading buffer (BioRad, #1610738, without SDS) was loaded onto a 5.5% native polyacrylamide gel (1.5 M Tris-HCl, Resolving Gel buffer, ProtoGel, 30% acrylamide, 10% APS, TEMED, without SDS) with native unstained protein marker (Invitrogen, LC0725). Gels were run at 120 V for 2 h followed by a transfer onto PVDF membrane in Tris-glycine-0.1% SDS transfer buffer at 200 mA/16 V overnight at 4 °C. Membranes were blocked in 5% nonfat dry milk in tris-buffered saline (TBS) and 0.1% Tween-20 and incubated overnight in mouse anti-HSP90 (H9010, Stressmarq SMC-107, 1:2000), rat anti-HSC70 (Enzo, ADI-SPA-815, 1:2000) or mouse anti-HOP (Enzo, SRA-1500, 1:2000). Membranes were incubated in respective horseradish peroxidase conjugated secondary antibodies (Thermo-Fischer) at room temperature for 1 h and developed for image quantification. Chemiluminescent signals were visualized using chemiluminescence detection system (Supersignal, Pierce). Blots were imaged with the Chemidoc Imager (BioRad). Optical density (OD) of protein bands were measured using

ImageJ (National Institutes of Health). OD of HMW bands (between 480 and 720kD for HSP90 and HSC70; between 250 and 300kD for HOP) were normalized to SDS PAGE measurements of associated monomeric protein and actin OD levels (described below).

2.4. Sodium dodecyl-sulfate (SDS)-PAGE Western Blot

20 μg of hippocampal protein samples and a molecular weight marker (Bio-Rad, Hercules, CA) were separated using SDS-PAGE. The resolved proteins were electrophoretically transferred to a PVDF membrane (Invitrogen, Carlsbad, CA). The membranes were blocked in 5% nonfat dry milk in tris-buffered saline (TBS) then probed with antibodies recognizing HSP90 (Stressmarq), HSC70 (Enzo), and HOP (Enzo) and incubated overnight at 4 °C. The following day, the membranes were incubated in their respective horseradish peroxidase conjugated secondary antibodies (Thermo-Fischer). Mouse or rabbit anti-actin (Sigma, 1:10,000) was used as a loading control. Between primary antibody incubations, membranes were stripped (RestoreTM PLUS, Thermo Fischer) and re-blocked. Proteins were visualized using a chemiluminescence detection system (Supersignal, Pierce). Blots were imaged with the Chemidoc Imager (BioRad). Optical density (OD) of monomeric protein bands were measured using ImageJ (NIH) and normalized to actin OD levels.

2.5. Statistics

Values are presented as the ratio of optical densities of samples as a percentage of sham (100%) for each time point. Data are presented as bar graphs with individual values showing the mean ± standard deviation (SD). Immunoblot data was compared using a two-way analysis of variance (ANOVA) to evaluate the effects of injury and biological sex at each time-point followed by *posthoc* Tukey's test, when appropriate. A p-value $p < 0.05$ was considered statistically significant for all tests. Statistical tests were completed using GraphPad Prism (GraphPad, La Jolla, CA).

3. Results

3.1. CCI significantly increases high molecular weight HSP90 expression at all time-points

At 24 hours, 1, 2 and 4 weeks post-injury HMW expression of HSP90, one of the central proteins within the epichaperome complex, was measured in the ipsilateral hippocampus by Native-PAGE and levels were normalized to monomeric (SDS) protein expression (Fig. 1A–H).

Changes in monomeric HSP90 expression was analyzed by two-way ANOVA to examine the effects of injury and sex at each time-point. At 24 hours post-injury, there is a significant main effect of injury ($p = 0.0054$), with no significant effect of sex and no significant interaction (Fig. 1I). At 1, 2 and 4 weeks post-injury, there was no significant main effect of injury or sex and no significant interaction in HSP90 monomeric expression (Fig. 1J, K, L).

Changes in HMW HSP90 expression was analyzed by two-way ANOVA to examine the effects of injury and sex at each time-point. At 24 hours post-injury, there is a significant main effect of injury ($p = 0.0002$), showing significantly higher HMW HSP90 expression

in the CCI group compared to sham (Fig. 1M). There is no significant effect of sex and no significant interaction. At 1 week post-injury, there is a significant main effect of injury (p = 0.0004), showing significantly higher HMW HSP90 expression in the CCI group compared to sham (Fig. 1N). There is no significant effect of sex and no significant interaction. At 2 weeks post-injury, there is a significant main effect of injury ($p < 0.0001$), showing significantly higher HMW HSP90 expression in the CCI group compared to sham (Fig. 1O). There is no significant effect of sex and no significant interaction. At 4 weeks post-injury, there is a significant main effect of injury ($p < 0.0001$), showing significantly higher HMW HSP90 expression in the CCI group compared to sham (Fig. 1P). There is no significant effect of sex and no significant interaction. Altogether, injury appears to increase HSP90 epichaperome expression in across all time-points with no differences between sexes.

3.2. CCI significantly increases high molecular weight HSC70 expression at all time-points

At 24 hours, 1, 2 and 4 weeks post-injury HMW expression of HSC70, another important hub protein within the epichaperome complex, was measured in the ipsilateral hippocampus by Native-PAGE and levels were normalized to monomeric protein expression (Fig. 2A–H).

Changes in monomeric HSC70 expression was analyzed by two-way ANOVA to examine the effects of injury and sex at each time-point. At 24 hours post-injury, there is a significant main effect of injury (p = 0.0279), showing significantly higher monomeric HSC70 expression in the CCI group compared to sham (Fig. 2I). There is no significant effect of sex and no significant interaction. At 1 week post-injury, there is a significant main effect of injury (p = 0.0025), showing significantly lower monomeric HSC70 expression in the CCI group compared to sham (Fig. 2J). There is no significant effect of sex and no significant interaction. At 2 and 4 weeks post-injury, there was no significant main effect of injury or sex and no significant interaction in HSC70 monomeric expression (Fig. 2K, L).

Changes in HMW HSC70 expression was analyzed by two-way ANOVA to examine the effects of injury and sex at each time-point. At 24 hours post-injury, there is a significant main effect of injury ($p < 0.0001$), significant main effect of sex (p = 0.0391) and a significant injury*sex interaction (p = 0.0391) (Fig. 2M). *Post-hoc* shows male animals have significantly higher HMW HSC70 expression after CCI compared to sham (p = 0.0002) while females show no significant difference in expression after CCI. Injured male animals have significantly higher HMW HSC70 expression compared to injured female animals (p = 0.0254), while there are no differences between the sexes between sham animals. At 1 week post-injury, there is a significant main effect of injury (p = 0.0004), showing significantly higher HMW HSC70 expression in the CCI group compared to sham (Fig. 2N). There is no significant effect of sex and no significant interaction. At 2 weeks post-injury, there is a significant main effect of injury (p = 0.0003), showing significantly higher HMW HSC70 expression in the CCI group compared to sham (Fig. 2O). There is no significant effect of sex and no significant interaction. At 4 weeks post-injury, there is a significant main effect of injury (p = 0.0004), significant main effect of sex (p = 0.0147) and a significant injury*sex interaction (p = 0.0145) (Fig. 2P). *Post-hoc* shows female animals have significantly higher HMW HSC70 expression after CCI compared to sham

($p = 0.0005$) while males show no significant difference in expression after CCI. Injured female animals have significantly higher HMW HSC70 expression compared to injured male animals ($p = 0.0059$), while there are no differences between the sexes between sham animals. Altogether, TBI appears to increase HSC70 epichaperome expression with distinct expression patterns for male and female animals at various time-points.

3.3. CCI significantly changes high molecular weight and monomeric HOP expression based on sex

At 24 hours, 1, 2 and 4 weeks post-injury HMW expression of HOP, a linking protein between HSP90 and HSC70, was measured in the ipsilateral hippocampus by Native-PAGE and levels were normalized to monomeric protein expression (Fig. 3A–H).

Changes in monomeric HOP expression was analyzed by two-way ANOVA to examine the effects of injury and sex at each time-point. At 24 hours post-injury, there was no significant main effect of injury or sex and no significant interaction in HOP monomeric expression (Fig. 3I). At 1 week post-injury, there is a significant main effect of injury ($p = 0.0005$), showing significantly lower monomeric HOP expression in the CCI group compared to sham (Fig. 3J). There is no significant effect of sex and no significant interaction. At 2 weeks post-injury, there is a significant main effect of sex ($p = 0.0005$) and a significant injury*sex interaction ($p = 0.0032$) (Fig. 3K). *Post-hoc* shows significantly lower monomeric HOP expression in the female CCI group. Similarly, 4 week post-injury, there is a significant main effect of sex ($p = 0.0302$) and a significant injury*sex interaction ($p = 0.0302$) (Fig. 3L). *Post-hoc* shows significantly lower monomeric HOP expression in the female CCI group.

Changes in HMW HOP expression was analyzed by two-way ANOVA to examine the effects of injury and sex at each time-point. At 24 hours post-injury, there is a significant main effect of injury ($p < 0.0001$), significant main effect of sex ($p = 0.0087$) and a significant injury*sex interaction ($p = 0.0087$) (Fig. 3M). *Post-hoc* shows male animals have significantly higher HMW HOP expression after CCI compared to sham ($p < 0.0001$) while females show no significant difference in expression after CCI. Injured male animals have significantly higher HMW HOP expression compared to injured female animals ($p = 0.0028$), while there are no differences between the sexes in sham animals. At 1 week post-injury, there is a significant main effect of injury ($p = 0.0012$), showing a significant increase in HMW HOP expression in the CCI group compared to sham (Fig. 3N). There is no significant effect of sex and no significant interaction. At 2 weeks post-injury, there is a significant main effect of injury ($p = 0.0003$), showing significantly higher HMW HOP expression in the CCI group compared to sham (Fig. 3O). There is no significant effect of sex and no significant interaction. At 4 weeks post-injury, there is a significant main effect of injury ($p = 0.0001$), showing significantly higher HMW HOP expression in the CCI group compared to sham (Fig. 3P). There is no significant effect of sex and no significant interaction. Altogether, TBI appears to increase HOP epichaperome expression with distinct expression patterns for male and female animals at various time-points.

4. Discussion

Formation of the epichaperome was initially discovered as a survival mechanism in tumors (Rodina et al., 2016), and later found in brain regions responsible for cognition in human and pre-clinical AD models (Inda et al., 2020). Given the connection between TBI and neurodegenerative diseases, this study aimed to examine epichaperome formation in an experimental model of TBI. We hypothesized that TBI would similarly increase. We measured high molecular weight expression of HSP90, HSC70 and HOP, key hub proteins within the epichaperome, 24 hours, 1, 2 and 4 weeks after CCI. We found TBI significantly increases epichaperome complex formation across all three proteins, independent of monomeric changes after injury.

Measurement of monomeric HSP90 and HSC70 protein levels generally replicated previous findings in TBI (Chen et al., 1998; Dutcher et al., 1998; Hayes et al., 1995; Lai et al., 2004; Michael et al., 2005; Raghupathi et al., 1995; Seidberg et al., 2003; Truettner et al., 1999, 2007). We found an increase in monomeric expression of HSP90 and HSC70 24 h after CCI By 2 weeks post-injury levels return to baseline and remained unchanged through 4 weeks post-injury. Conversely, monomeric HOP expression was unchanged early, however had a significant drop in expression at 1 week post-injury and remained below baseline through 4 weeks. Data suggests, that regardless of monomeric levels, especially during decreases, epichaperome formation remains increased after CCI. This divergence highlights the importance of distinguishing HSPs within the epichaperome from their monomeric form.

HSP90, the most-abundant HSP and primary epichaperome hub protein, had the most consistent injury response, showing steady increases across all time-points in both sexes. HSC70 and HOP appeared to display a much higher response early that leveled off to quantities as HSP90 by 2 weeks post-injury. This suggests that HSC70 and HOP may be more sensitive to hallmark TBI neuronal pathologies such as inflammation, oxidative stress, vascular disruption, and/or excitotoxicity (Chiu et al., 2016; Kalimon and Sullivan, 2021; Kenney et al., 2016; Krishnamurthy and Laskowitz, 2016). Across all proteins, the 1 week time-point showed a relatively larger degree of variability compared to the other time-points, reflecting a possible inflection point of compensatory mechanisms or reflecting heterogeneity of TBI outcomes. The epichaperome complexes provide a lens into known TBI pathologies while also providing a unique perspective into a contributing pathological mechanism.

While no sex differences were observed in HSP90 expression, HSC70 and HOP demonstrated sex differences, particularly at the 24 hours and 4 week time-point. Male animals showed significantly higher epichaperome formation early. Conversely, female animals showed significantly higher epichaperome formation late. This pattern parallels previous work examining behavioral and molecular sex differences after experimental TBI. For example, males demonstrate larger neuroinflammatory response than females at early time-points (Doran et al., 2019; Villapol et al., 2017). Females have faster baseline recovery in motor performance acutely after injury (Doran et al., 2019; Wagner et al., 2004). Similarly, another study found males had peak protein degradative neurodegenerative histopathology at 3 days post-injury, while female animals peaked at 14 days post-injury

(Kupina et al., 2003) or at 4 weeks (Hall et al., 2005). It is unknown whether increased risk of developing neurodegenerative disease after TBI is modulated by biological sex (Biegon, 2021), however epichaperome assist decoding sex differences and identifying neurodegenerative associated pathology in acute and chronic time-points post-injury.

The link between TBI and development of dementia and neurodegenerative disease is unclear. Current hypotheses postulate that TBI-induced axonal injury, blood brain barrier breakdown and rising neuroinflammation contribute to the production of hallmark pathological proteins such as amyloid beta and tau. HSP90 and its co-chaperones are responsible for folding tau or hyper phosphorylated tau while HSP70 chaperone complex mediates tau degradation (Dickey et al., 2007; Thompson et al., 2012). The switch of the chaperome to the epichaperome precedes hippocampal tau pathology in the tau P301S (PS19) transgenic mice by a few months and pharmacological reduction of the epichaperome reduces expression soluble, hyperphosphorylated and oligomeric tau species (Inda et al., 2020). TBI-induced increases in epichaperome formation, particularly through sub-acute time-points post-injury, could be a link between TBI and neurodegenerative disease. Studies not examining the epichaperome directly, but looking at proteostasis, note changes in tau kinase activity, stress granule assembly APP biosynthesis (Wu et al., 2022). This might allude to downstream impacts of epichaperome formation. Connection of the TBI-induced epichaperome and downstream development of tauopathy would be an interesting future direction.

Pharmacological or transgenic therapies that activate or increase expression of HSPs have conferred some therapeutic benefit, specifically through reducing inflammation and apoptosis (Eroglu et al., 2014; Gu et al., 2016; Kim et al., 2013, 2015). However, these studies have not evaluated molecular and behavior improvements beyond 14 days post-injury. The epichaperome can be dismantled pharmacologically and has been tested in animals and humans across various disorders. Icapamespib (also known as PU-AD or PUHZ-151) is a blood brain barrier penetrable small molecular that is deigned to specifically target and inhibit epichaperome formation in diseases cells (Bolaender et al., 2021). It is highly selective for the conformationally altered HSP90 adenosine triphosphate binding site. Importantly, icapamespib does not change HPS90 monomeric expression or interfere with healthy chaperome function. In pre-clinical models of early and late-stage AD, epichaperome inhibition by chronic, intermittent administration of PU-AD corrected the activity of synaptic protein networks, restored synaptic plasticity and improved learning and memory behaviors (Inda et al., 2020). In a neuron-astrocyte organoid tauopathy model, epichaperome disruption with PU-H71 reduced expression of misfolded and hyperphosphorylated tau and decreased expression of neuronal cell death markers. Additionally, PU-H71 treatment shifted reactive astrocyte phenotype towards a protective astrocytic form and a similar shift was observed in transcriptomic analysis of the neuroinflammatory profile (Rickner et al., 2022). This suggests observed TBI-mediated epichaperome formation may span across cell-types and exacerbate or mediate canonical TBI inflammatory pathology. Clinical trials have determined that this drug is able to be safely used in humans for long periods of time/chronic administration (Silverman et al., 2022). Understanding the timeline and severity of epichaperome formation after TBI can lead to targeting intervention by these established therapies. Furthermore, beyond

therapeutics, the use of epichaperome inhibitors, such as PU-AD, provide a valuable tool to understand the breadth of epichaperome mediated protein network dysfunction after TBI.

While HSP90, HSC70 and HOP are the primary indicators of epichaperome formation, there are a host of other proteins that are recruited into this pathological complex, including HSP110 and CDC37. The immunoblot method limits us to measuring one protein at a time which is not efficient for understanding the network of proteins involved. Innovative and unbiased proteomics approach uses epichaperome targeted bait to not only understand the contents of the epichaperome, but the degree of interaction between proteins within the complex (Inda et al., 2020). Moreover, this method limits the identification of pathological high molecular weight HSP90 across various cell types such as glial cells or within specific cellular compartments within the neuron. In a murine model of AD, the epichaperome was detected primarily in the hippocampus, but also in the entorhinal cortex and amygdala (Inda et al., 2020). Cognitive impairments due to TBI involve dysfunction across brain regions beyond the temporal lobe (Paterno et al., 2017). Characterization of epichaperome formation various brain regions, particularly in diffuse experimental TBI models such as fluid percussion, could reveal the connection between TBI injury mechanisms and the epichaperome.

5. Conclusions

Controlled cortical impact significantly increases epichaperome protein expression of HSP90, HSC70 and HOP in the ipsilateral hippocampus up to 4 weeks post-injury. This finding suggests a potential link between acute and sub-acute injury cascades and neurodegenerative pathologies. Future studies pharmacologically dismantling the epichaperome could be a therapeutic target for treating TBI.

Supplementary Material

Refer to Web version on PubMed Central for supplementary material.

Acknowledgements

We thank Dr. Margaret Young for administrative support.

Funding and disclosure

This work was supported by UPMC Neurotrauma Endowed Chair Fund (CED).

Data availability

Data will be made available on request.

References

Balchin D, Hayer-Hartl M, Hartl FU, 2016. In vivo aspects of protein folding and quality control. Science 353, aac4354. 10.1126/science.aac4354. [PubMed: 27365453]

Biegon A, 2021. Considering biological sex in traumatic brain injury. Front. Neurol. 12.

Bolaender A, Zatorska D, He H, Joshi S, Sharma S, Digwal CS, Patel HJ, Sun W, Imber BS, Ochiana SO, Patel MR, Shrestha L, Shah Smit K, Wang S, Karimov R, Tao H, Patel PD, Martin AR, Yan P, Panchal P, Almodovar J, Corben A, Rimner A, Ginsberg SD, Lyashchenko S, Burnazi E, Ku A, Kalidindi T, Lee SG, Grkovski M, Beattie BJ, Zanzonico P, Lewis JS, Larson S, Rodina A, Pillarsetty N, Tabar V, Dunphy MP, Taldone T, Shimizu F, Chiosis G, 2021. Chemical tools for epichaperome-mediated interactome dysfunctions of the central nervous system. Nat. Commun. 12, 4669. 10.1038/s41467-021-24821-2. [PubMed: 34344873]

Bramlett HM, Dietrich WD, 2015. Long-term consequences of traumatic brain injury: current status of potential mechanisms of injury and neurological outcomes. J. Neurotrauma 32, 1834–1848. 10.1089/neu.2014.3352. [PubMed: 25158206]

Brett BL, Gardner RC, Godbout J, Dams-O'Connor K, Keene CD, 2022. Traumatic brain injury and risk of neurodegenerative disorder. Biol. Psychiatry, Traumatic Brain Injury and Mental Health 91, 498–507. 10.1016/j.biopsych.2021.05.025.

Chen M, Clark RS, Kochanek PM, Chen J, Schiding JK, Stetler RA, Simon RP, Graham SH, 1998. 72-kDa heat shock protein and mRNA expression after controlled cortical impact injury with hypoxemia in rats. J. Neurotrauma 15, 171–181. 10.1089/neu.1998.15.171. [PubMed: 9528917]

Chiosis G, Digwal CS, Trepel JB, Neckers L, 2023. Structural and functional complexity of HSP90 in cellular homeostasis and disease. Nat. Rev. Mol. Cell Biol. 1–19 10.1038/s41580-023-00640-9. [PubMed: 36319695]

Chiu C-C, Liao Y-E, Yang L-Y, Wang Jing-Ya, Tweedie D, Karnati HK, Greig NH, Wang Jia-Yi, 2016. Neuroinflammation in animal models of traumatic brain injury. J. Neurosci. Methods 272, 38–49. 10.1016/j.jneumeth.2016.06.018. [PubMed: 27382003]

Cora MC, Kooistra L, Travlos G, 2015. Vaginal cytology of the laboratory rat and mouse: review and criteria for the staging of the estrous cycle using stained vaginal smears. Toxicol. Pathol. 43, 776–793. 10.1177/0192623315570339. [PubMed: 25739587]

Cruz-Haces M, Tang J, Acosta G, Fernandez J, Shi R, 2017. Pathological correlations between traumatic brain injury and chronic neurodegenerative diseases. Transl. Neurodegener. 6, 20. 10.1186/s40035-017-0088-2. [PubMed: 28702179]

Dickey CA, Kamal A, Lundgren K, Klosak N, Bailey RM, Dunmore J, Ash P, Shoraka S, Zlatkovic J, Eckman CB, Patterson C, Dickson DW, Nahman NS, Hutton M, Burrows F, Petrucelli L, 2007. The high-affinity HSP90-CHIP complex recognizes and selectively degrades phosphorylated tau client proteins. J. Clin. Invest. 117, 648–658. 10.1172/JCI29715. [PubMed: 17304350]

Doran SJ, Ritzel RM, Glaser EP, Henry RJ, Faden AI, Loane DJ, 2019. Sex differences in acute Neuroinflammation after experimental traumatic brain injury are mediated by infiltrating myeloid cells. J. Neurotrauma 36, 1040–1053. 10.1089/neu.2018.6019. [PubMed: 30259790]

Dutcher SA, Underwood BD, Walker PD, Diaz FG, Michael DB, 1998. Patterns of heat-shock protein 70 biosynthesis following human traumatic brain injury. J. Neurotrauma 15, 411–420. 10.1089/neu.1998.15.411. [PubMed: 9624626]

Eroglu B, Kimbler DE, Pang J, Choi J, Moskophidis D, Yanasak N, Dhandapani KM, Mivechi NF, 2014. Therapeutic inducers of the HSP70/HSP110 protect mice against traumatic brain injury. J. Neurochem. 130, 626–641. 10.1111/jnc.12781. [PubMed: 24903326]

Fortress AM, Avcu P, Wagner AK, Dixon CE, Pang KCH, 2019. Experimental traumatic brain injury results in estrous cycle disruption, neurobehavioral deficits, and impaired GSK3β/β-catenin signaling in female rats. Exp. Neurol. 315, 42–51. 10.1016/j.expneurol.2019.01.017. [PubMed: 30710530]

Ginsberg SD, Joshi S, Sharma S, Guzman G, Wang T, Arancio O, Chiosis G, 2021. The penalty of stress—Epichaperomes negatively reshaping the brain in neurodegenerative disorders. J. Neurochem. 159, 958–979. 10.1111/jnc.15525. [PubMed: 34657288]

Ginsberg SD, Neubert TA, Sharma S, Digwal CS, Yan P, Timbus C, Wang T, Chiosis G, 2022. Disease-specific interactome alterations via epichaperomics: the case for Alzheimer's disease. FEBS J. 289, 2047–2066. 10.1111/febs.16031. [PubMed: 34028172]

Ginsberg SD, Sharma S, Norton L, Chiosis G, 2023. Targeting stressor-induced dysfunctions in protein–protein interaction networks via epichaperomes. Trends Pharmacol. Sci. 44, 20–33. 10.1016/j.tips.2022.10.006. [PubMed: 36414432]

Graham NS, Sharp DJ, 2019. Understanding neurodegeneration after traumatic brain injury: from mechanisms to clinical trials in dementia. J. Neurol. Neurosurg. Psychiatry 90, 1221–1233. 10.1136/jnnp-2017-317557. [PubMed: 31542723]

Gu Y, Chen J, Wang T, Zhou C, Liu Z, Ma L, 2016. Hsp70 inducer, 17-allylamino-demethoxygeldanamycin, provides neuroprotection via anti-inflammatory effects in a rat model of traumatic brain injury. Exp. Ther. Med. 12, 3767–3772. 10.3892/etm.2016.3821. [PubMed: 28101166]

Hall ED, Gibson TR, Pavel KM, 2005. Lack of a gender difference in post-traumatic neurodegeneration in the mouse controlled cortical impact injury model. J. Neurotrauma 22, 669–679. 10.1089/neu.2005.22.669. [PubMed: 15941376]

Harper JW, Bennett EJ, 2016. Proteome complexity and the forces that drive proteome imbalance. Nature 537, 328–338. 10.1038/nature19947. [PubMed: 27629639]

Hayes R, Yang K, Raghupathi R, Mcintosh TK, 1995. Changes in gene expression following traumatic brain injury in the rat. J. Neurotrauma 12, 779–790. 10.1089/neu.1995.12.779. [PubMed: 8594207]

Inda MC, Joshi S, Wang T, Bolaender A, Gandu S, Koren III J, Che AY, Taldone T, Yan P, Sun W, Uddin M, Panchal P, Riolo M, Shah S, Barlas A, Xu K, Chan LYL, Gruzinova A, Kishinevsky S, Studer L, Fossati V, Noggle SA, White JR, de Stanchina E, Sequeira S, Anthoney KH, Steele JW, Manova-Todorova K, Patil S, Dunphy MP, Pillarsetty N, Pereira AC, Erdjument-Bromage H, Neubert TA, Rodina A, Ginsberg SD, De Marco Garcia N, Luo W, Chiosis G, 2020. The epichaperome is a mediator of toxic hippocampal stress and leads to protein connectivity-based dysfunction. Nat. Commun. 11, 319. 10.1038/s41467-019-14082-5. [PubMed: 31949159]

Joshi S, Wang T, Araujo TLS, Sharma S, Brodsky JL, Chiosis G, 2018. Adapting to stress — chaperome networks in cancer. Nat. Rev. Cancer 18, 562–575. 10.1038/s41568-018-0020-9. [PubMed: 29795326]

Kalimon OJ, Sullivan PG, 2021. Sex differences in mitochondrial function following a controlled cortical impact traumatic brain injury in rodents. Front. Mol. Neurosci. 14, 753946 10.3389/fnmol.2021.753946. [PubMed: 34720875]

Kaushik S, Cuervo AM, 2015. Proteostasis and aging. Nat. Med. 21, 1406–1415. 10.1038/nm.4001. [PubMed: 26646497]

Kenney K, Amyot F, Haber M, Pronger A, Bogoslovsky T, Moore C, Diaz-Arrastia R, 2016. Cerebral vascular injury in traumatic brain injury. Exp. Neurol Traum. Brain Injury 275, 353–366. 10.1016/j.expneurol.2015.05.019.

Kim JY, Kim N, Zheng Z, Lee JE, Yenari MA, 2013. The 70kD heat shock protein protects against experimental traumatic brain injury. Neurobiol. Dis. 58, 289–295. 10.1016/j.nbd.2013.06.012. [PubMed: 23816752]

Kim N, Kim JY, Yenari MA, 2015. Pharmacological induction of the 70 kDa heat shock protein protects against brain injury. Neuroscience 284, 912–919. 10.1016/j.neuroscience.2014.11.010. [PubMed: 25446362]

Kishinevsky S, Wang T, Rodina A, Chung SY, Xu C, Philip J, Taldone T, Joshi S, Alpaugh ML, Bolaender A, Gutbier S, Sandhu D, Fattahi F, Zimmer B, Shah SK, Chang E, Inda C, Koren J, Saurat NG, Leist M, Gross SS, Seshan VE, Klein C, Tomishima MJ, Erdjument-Bromage H, Neubert TA, Henrickson RC, Chiosis G, Studer L, 2018. HSP90-incorporating chaperome networks as biosensor for disease-related pathways in patient-specific midbrain dopamine neurons. Nat. Commun. 9, 4345. 10.1038/s41467-018-06486-6. [PubMed: 30341316]

Krishnamurthy K, Laskowitz DT, 2016. Cellular and molecular mechanisms of secondary neuronal injury following traumatic brain injury. In: Laskowitz D, Grant G (Eds.), Translational Research in Traumatic Brain Injury, Frontiers in Neuroscience. CRC Press/Taylor and Francis Group, Boca Raton (FL).

Kupina NC, Detloff MR, Bobrowski WF, Snyder BJ, Hall ED, 2003. Cytoskeletal protein degradation and neurodegeneration evolves differently in males and females following experimental head injury. Exp. Neurol. 180, 55–73. 10.1016/S0014-4886(02)00048-1. [PubMed: 12668149]

Lai Y, Kochanek PM, Adelson PD, Janesko K, Ruppel RA, Clark RSB, 2004. Induction of the stress response after inflicted and non-inflicted traumatic brain injury in infants and children. J. Neurotrauma 21, 229–237. 10.1089/089771504322972022. [PubMed: 15115598]

Lindberg I, Shorter J, Wiseman RL, Chiti F, Dickey CA, McLean PJ, 2015. Chaperones in Neurodegeneration. J. Neurosci. 35, 13853–13859. 10.1523/JNEUROSCI.2600-15.2015. [PubMed: 26468185]

Michael DB, Byers DM, Irwin LN, 2005. Gene expression following traumatic brain injury in humans: analysis by microarray. J. Clin. Neurosci. 12, 284–290. 10.1016/j.jocn.2004.11.003. [PubMed: 15851083]

Paterno R, Folweiler KA, Cohen AS, 2017. Pathophysiology and treatment of memory dysfunction after traumatic brain injury. Curr. Neurol. Neurosci. Rep. 17, 52. 10.1007/s11910-017-0762-x. [PubMed: 28500417]

Raghupathi R, Welsh FA, Lowenstein DH, Gennarelli TA, McIntosh TK, 1995. Regional induction of c-Fos and heat shock Protein-72 mRNA following fluid-percussion brain injury in the rat. J. Cereb. Blood Flow Metab. 15, 467–473. 10.1038/jcbfm.1995.58. [PubMed: 7714005]

Rickner HD, Jiang L, Hong R, O'Neill NK, Mojica CA, Snyder BJ, Zhang L, Shaw D, Medalla M, Wolozin B, Cheng CS, 2022. Single cell transcriptomic profiling of a neuron-astrocyte assembloid tauopathy model. Nat. Commun. 13, 6275. 10.1038/s41467-022-34005-1. [PubMed: 36271092]

Rodina A, Wang T, Yan P, Gomes ED, Dunphy MPS, Pillarsetty N, Koren J, Gerecitano JF, Taldone T, Zong H, Caldas-Lopes E, Alpaugh M, Corben A, Riolo M, Beattie B, Pressl C, Peter RI, Xu C, Trondl R, Patel HJ, Shimizu F, Bolaender A, Yang C, Panchal P, Farooq MF, Kishinevsky S, Modi S, Lin O, Chu F, Patil S, Erdjument-Bromage H, Zanzonico P, Hudis C, Studer L, Roboz GJ, Cesarman E, Cerchietti L, Levine R, Melnick A, Larson SM, Lewis JS, Guzman ML, Chiosis G, 2016. The epichaperome is an integrated chaperome network that facilitates tumour survival. Nature 538, 397–401. 10.1038/nature19807. [PubMed: 27706135]

Seidberg NA, Clark RSB, Zhang X, Lai Y, Chen M, Graham SH, Kochanek PM, Watkins SC, Marion DW, 2003. Alterations in inducible 72-kDa heat shock protein and the chaperone cofactor BAG-1 in human brain after head injury. J. Neurochem. 84, 514–521. 10.1046/j.1471-4159.2003.01547.x. [PubMed: 12558971]

Silverman MH, Duggan S, Bardelli G, Sadler B, Key C, Medlock M, Reynolds L, Wallner B, 2022. Safety, tolerability and pharmacokinetics of Icapamespib, a selective Epichaperome inhibitor, in healthy adults. J. Prev Alzheimers Dis. 9, 635–645. 10.14283/jpad.2022.71. [PubMed: 36281667]

Simon DW, McGeachy MJ, Bayır H, Clark RSB, Loane DJ, Kochanek PM, 2017. The far-reaching scope of neuroinflammation after traumatic brain injury. Nat. Rev. Neurol. 13, 171–191. 10.1038/nrneurol.2017.13. [PubMed: 28186177]

Smith DH, Uryu K, Saatman KE, Trojanowski JQ, McIntosh TK, 2003. Protein accumulation in traumatic brain injury. NeuroMolecular Med. 4, 59–72. 10.1385/NMM:4:1-2:59. [PubMed: 14528053]

Tai W, Guzman ML, Chiosis G, 2016. The epichaperome: the power of many as the power of one. Oncoscience 3, 266–267. 10.18632/oncoscience.321. [PubMed: 28050576]

Thompson AD, Scaglione KM, Prensner J, Gillies AT, Chinnaiyan A, Paulson HL, Jinwal UK, Dickey CA, Gestwicki JE, 2012. Analysis of the tau-associated proteome reveals that exchange of Hsp70 for Hsp90 is involved in tau degradation. ACS Chem. Biol 7, 1677–1686. 10.1021/cb3002599. [PubMed: 22769591]

Truettner J, Schmidt-Kastner R, Busto R, Alonso O, Loor JY, Dietrich WD, Ginsberg MD, 1999. Expression of brain-derived neurotrophic factor, nerve growth factor, and heat shock protein HSP70 following fluid percussion brain injury in rats. J. Neurotrauma 16, 471–486. 10.1089/neu.1999.16.471. [PubMed: 10391364]

Truettner JS, Hu B, Alonso OF, Bramlett HM, Kokame K, Dietrich WD, 2007. Subcellular stress response after traumatic brain injury. J. Neurotrauma 24, 599–612. 10.1089/neu.2006.0186. [PubMed: 17439344]

Villapol S, Loane DJ, Burns MP, 2017. Sexual dimorphism in the inflammatory response to traumatic brain injury. Glia 65, 1423–1438. 10.1002/glia.23171. [PubMed: 28608978]

Wagner AK, Willard LA, Kline AE, Wenger MK, Bolinger BD, Ren D, Zafonte RD, Dixon CE, 2004. Evaluation of estrous cycle stage and gender on behavioral outcome after experimental traumatic brain injury. Brain Res. 998, 113–121. 10.1016/j.brainres.2003.11.027. [PubMed: 14725974]

Wu L, Kalish BT, Finander B, Cao T, Jin G, Yahya T, Levy ES, Kukreja B, LaRovere ES, Chung JY, Lo EH, Brown-Whalen A, Khoury JE, Kaplan DL, Whalen MJ, 2022. Repetitive mild closed head injury in adolescent mice is associated with impaired proteostasis, neuroinflammation, and tauopathy. J. Neurosci. 42, 2418–2432. 10.1523/JNEUROSCI.0682-21.2021. [PubMed: 35105673]

Yan P, Patel HJ, Sharma S, Corben A, Wang T, Panchal P, Yang C, Sun W, Araujo TL, Rodina A, Joshi S, Robzyk K, Gandu S, White JR, de Stanchina E, Modi S, Janjigian YY, Hill EG, Liu B, Erdjument-Bromage H, Neubert TA, Que NLS, Li Z, Gewirth DT, Taldone T, Chiosis G, 2020. Molecular stressors engender protein connectivity dysfunction through aberrant N-glycosylation of a chaperone. Cell Rep. 31, 107840 10.1016/j.celrep.2020.107840. [PubMed: 32610141]

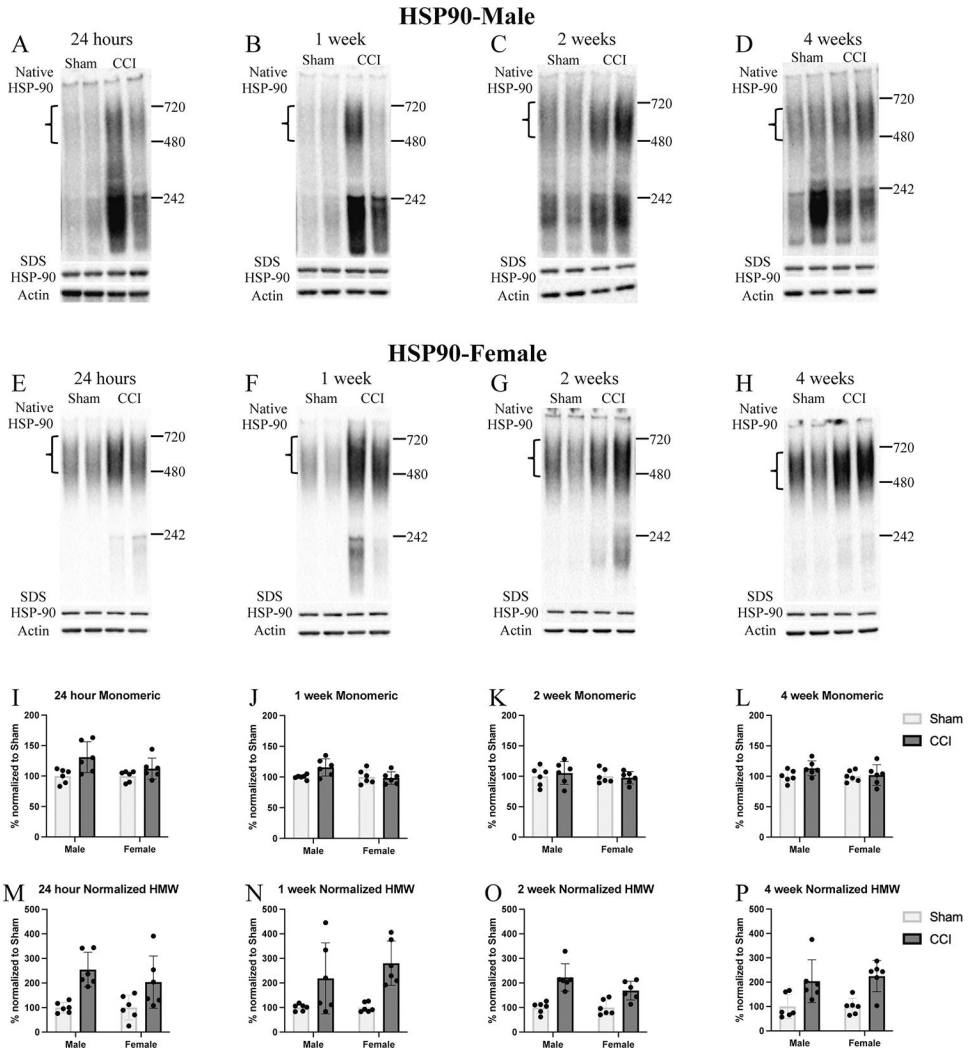

Fig. 1.

CCI significantly increases high molecular weight HSP90 expression at all time-points. Protein expression of HSP90 within the epichaperome was measured by native-PAGE (high molecular weight; HMW) and SDS-PAGE (monomer) after sham or CCI injury in male (A-D) and female (*E*-H) animals 24 hours to 4 weeks post-injury. Bracket shows HMW expression measured for optical density analysis. Representative $n = 2$ animals per group are shown ($N = 6$ total animals per group). Bar graphs show quantification of monomeric (I-L) and HSP90 HMW expression normalized to monomeric and beta-actin (M-P) in male and female animals after sham or CCI injury. Data is represented as mean ± standard deviation and normalized to corresponding sham group. Two-way ANOVA was used to analyze injury and sex effects at each timepoint. ## $p < 0.01$, ### $p < 0.001$, #### $p < 0.0001$ compared to sham animals (overall injury effect). No *post hoc* comparisons are displayed.

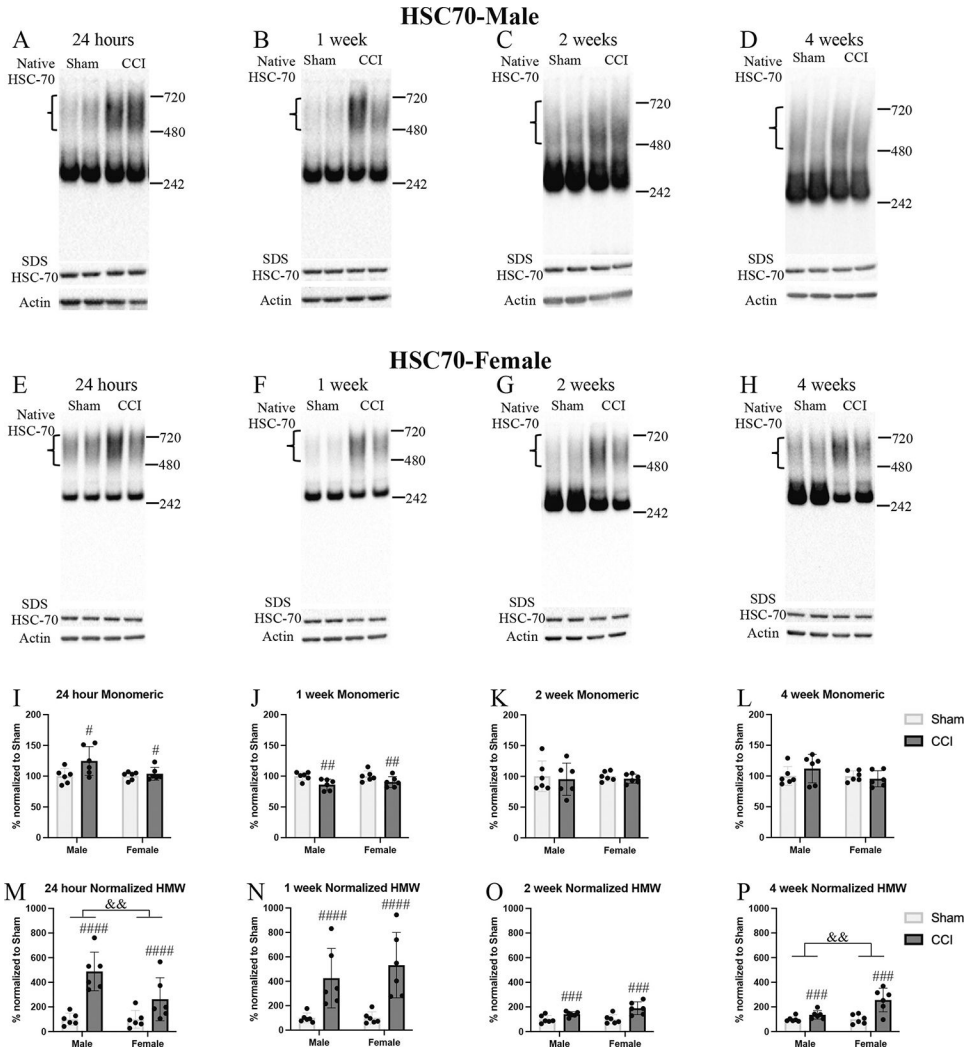

Fig. 2.

CCI significantly increases high molecular weight HSC70 expression at all time-points. Protein expression of HSC70 within the epichaperome was measured by native-PAGE (high molecular weight; HMW) and SDS-PAGE (monomer) after sham or CCI injury in male (A-D) and female (E-H) animals 24 hours to 4 weeks post-injury. Bracket shows high molecular weight (HMW) expression measured for optical density analysis. Representative n = 2 animals per group are shown (N = 6 total animals per group). Bar graphs show quantification of monomeric (I-L) and HMW HSC70 expression normalized to monomeric and beta-actin (M-P) in male and female animals after sham or CCI injury. Data is represented as mean ± standard deviation and normalized to corresponding sham group. Two-way ANOVA was used to analyze injury and sex effects at each timepoint. # $p <$ 0.05, ## p < 0.01, ### p < 0.001, #### p < 0.0001 compared to sham animals (overall injury effect); && p < 0.01 compared to male animals (overall sex effect). No *post hoc* comparisons are displayed.

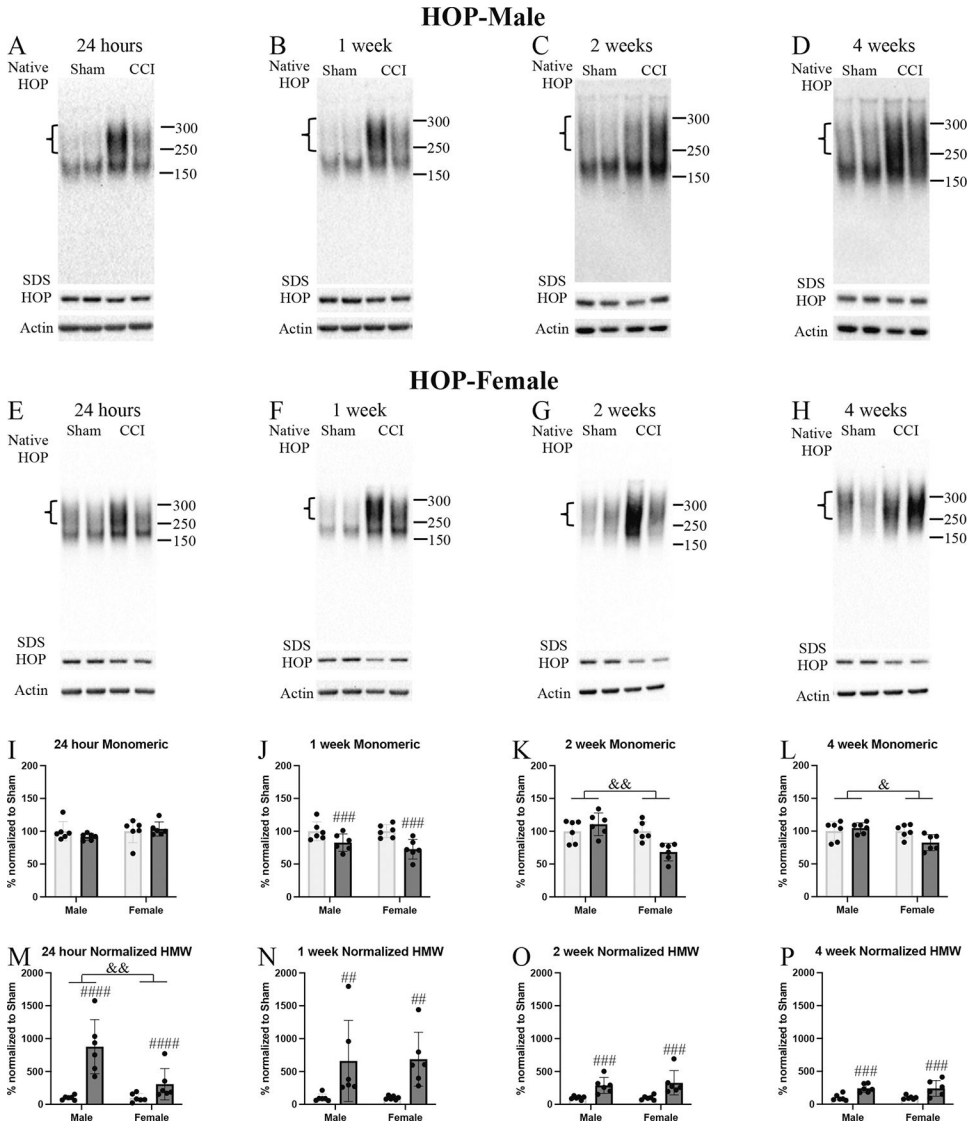

Fig. 3.

CCI significantly changes high molecular weight and monomeric HOP expression based on sex. Protein expression of HOP within the epichaperome was measured by native-PAGE (high molecular weight; HMW) and SDS-PAGE (monomer) after sham or CCI injury in male (A-D) and female (E-H) animals 24 hours to 4 weeks post-injury. Bracket shows high molecular weight (HMW) expression measured for optical density analysis. Representative n = 2 animals per group are shown (N = 6 total animals per group). Bar graphs show quantification of monomeric (I-L) and HMW HOP expression normalized to monomeric and beta-actin (M-P) in male and female animals after sham or CCI injury. Data is represented as mean ± standard deviation and normalized to corresponding sham group. Two-way ANOVA was used to analyze injury and sex effects at each timepoint. ## $p < 0.01$, ### $p < 0.001$, #### $p < 0.0001$ compared to sham animals (overall injury effect); & $p < 0.05$, && $p < 0.01$ compared to male animals (overall sex effect). No *post hoc* comparisons are displayed.